AFRL-RX-WP-TP-2010-4071

SLIP ACTIVITY IN SINGLE GRAINS EXTRACTED FROM POLYCRYSTALLINE SPECIMEN BY X-RAY LINE BROADENING (Preprint)

Ayman A. Salem and S. Lee Semiatin

Processing Section
Metals Branch

Tamás Ungár, Gábor Ribárik, and Levente Balogh

Eötvös University Budapest

Gavin Vaughan

European Synchrotron Research Facility

JANUARY 2010
Interim Report

AIR FORCE RESEARCH LABORATORY
MATERIALS AND MANUFACTURING DIRECTORATE
WRIGHT-PATTERSON AIR FORCE BASE, OH 45433-7750
AIR FORCE MATERIEL COMMAND
UNITED STATES AIR FORCE

REPORT DOCUMENTATION PAGE

Form Approved
OMB No. 0704-0188

1. REPORT DATE *(DD-MM-YY)*	2. REPORT TYPE	3. DATES COVERED *(From - To)*
January 2010	Journal Article Preprint	01 January 2010 – 01 January 2010

4. TITLE AND SUBTITLE
SLIP ACTIVITY IN SINGLE GRAINS EXTRACTED FROM POLYCRYSTALLINE SPECIMEN BY X-RAY LINE BROADENING (Preprint)

5a. CONTRACT NUMBER
IN HOUSE

5b. GRANT NUMBER

5c. PROGRAM ELEMENT NUMBER
62102F

6. AUTHOR(S)
Ayman A. Salem and S. Lee Semiatin (Metals Branch, Processing Section (AFRL/RXLMP))
Tamás Ungár, Gábor Ribárik, and Levente Balogh (Eötvös University Budapest)
Gavin Vaughan (European Synchrotron Research Facility)

5d. PROJECT NUMBER
4347

5e. TASK NUMBER
RG

5f. WORK UNIT NUMBER
M02R2000

7. PERFORMING ORGANIZATION NAME(S) AND ADDRESS(ES)

Processing Section (AFRL/RXLMP)
Metals Branch , Metals, Ceramics, and Nondestructive Evaluation Division
Materials and Manufacturing Directorate, Air Force Research Laboratory
Wright-Patterson Air Force Base, OH 45433-7750
Air Force Materiel Command, United States Air Force

Eötvös University Budapest
Department of Materials Physics

European Synchrotron Research Facility

8. PERFORMING ORGANIZATION REPORT NUMBER
AFRL-RX-WP-TP-2010-4071

9. SPONSORING/MONITORING AGENCY NAME(S) AND ADDRESS(ES)

Air Force Research Laboratory
Materials and Manufacturing Directorate
Wright-Patterson Air Force Base, OH 45433-7750
Air Force Materiel Command
United States Air Force

10. SPONSORING/MONITORING AGENCY ACRONYM(S)
AFRL/RXLMP

11. SPONSORING/MONITORING AGENCY REPORT NUMBER(S)
AFRL-RX-WP-TP-2010-4071

12. DISTRIBUTION/AVAILABILITY STATEMENT
Approved for public release; distribution unlimited.

13. SUPPLEMENTARY NOTES
PAO case number 88 ABW-2009-5026, cleared 03 December 2009. This work was funded in whole or in part by Department of the Air Force work unit M02R2000. The U.S. Government has for itself and others acting on its behalf an unlimited, paid-up, nonexclusive, irrevocable worldwide license to use, modify, reproduce, release, perform, display, or disclose the work by or on behalf of the U. S. Government. Submitted to Science Journal. Paper contains color.

14. ABSTRACT
Slip activity, Burgers vector populations, and dislocation densities were determined by X-ray line-profile analysis of peaks from individual grains in a bulk polycrystalline sample. The method was tested at the focused X-ray beamline ID11 at the European Synchrotron Research Facility (ESRF) in Grenoble, France and was applied to a bulk commercial-purity titanium specimen for which slip activity was determined for 49 single grains. The most-active slip systems were of <a> and <c+a> type, and the orientation of the stresses acting on these slip systems revealed a spread due to the effect of neighborhood grains on plastic response. The new x-ray method can provide input for crystal-plasticity analyses and permits experimental verification of the results of numerical calculations which was not possible before.

15. SUBJECT TERMS
slip activity, Burgers vector populations, dislocation densities, polycrystalline sample

16. SECURITY CLASSIFICATION OF:			17. LIMITATION OF ABSTRACT:	18. NUMBER OF PAGES	19a. NAME OF RESPONSIBLE PERSON (Monitor)
a. REPORT	b. ABSTRACT	c. THIS PAGE			Sheldon L. Semiatin
Unclassified	Unclassified	Unclassified	SAR	28	19b. TELEPHONE NUMBER *(Include Area Code)* N/A

Standard Form 298 (Rev. 8-98)
Prescribed by ANSI Std. Z39-18

Slip activity in single grains extracted from polycrystalline specimen by X-ray line broadening

Tamás Ungár[1], Gábor Ribárik[1], Levente Balogh[1], Ayman A. Salem[2], S. Lee Semiatin[2], and Gavin Vaughan[3]

[1]Department of Materials Physics, Eötvös University Budapest, H-1518, POB 32, Budapest, Hungary

[2]Air Force Research Laboratory, Materials and Manufacturing Directorate, Wright-Patterson Air Force Base, OH 45433 USA

[3] European Synchrotron Research Facility, B. P. 220, F - 38043, Grenoble cedex, France

One-sentence summary

A synchrotron X-ray line profile analysis method is developed for extracting slip activity and Burgers vector population within individual grains from a bulk polycrystalline material.

Abstract

Slip activity, Burgers vector populations, and dislocation densities were determined by X-ray line-profile analysis of peaks from individual grains in a bulk polycrystalline sample. The method was tested at the focused X-ray beamline ID11 at the European Synchrotron Research Facility (ESRF) in Grenoble, France and was applied to a bulk commercial-purity titanium specimen for which slip activity was determined for 49 single grains. The most-active slip systems were of <a> and <c+a> type, and the orientation of the stresses acting on these slip systems revealed a spread due to the effect of neighborhood grains on plastic response. The new x-ray method can provide input for crystal-plasticity analyses and permits experimental verification of the results of numerical calculations which was not possible before.

The plastic response of polycrystalline materials is a key issue for both the development of structural materials and for understanding the plastic behavior of crystalline minerals constituting different layers, as in the earth's mantle. In this work, the methods developed for differentiating the contributions of different grains in a polycrystalline sample (see e.g., [1] for a recent review) are extended to quantify the substructure within the individual grains in a bulk polycrystalline aggregate in terms of active slip systems, Burgers vectors, and dislocation densities. These properties are determined by X-ray line profile analysis of peaks from individual grains of a bulk polycrystalline commercial-purity titanium (CP-Ti) specimen using the focused X-ray beamline ID11 at the European Synchrotron Research Facility (ESRF) in Grenoble, France. Previously, a dislocation model of strain anisotropy has been developed and applied to determine the densities, arrangements, and edge or screw character of dislocations in cubic materials [2,S1,S2]. In polycrystalline materials, however, measurements averaged over many grains mask the important information needed to describe deformation at the grain scale [S2]. In order to quantify the plastic response of bulk polycrystalline materials based on a multiscale model one has to know which slip systems are active within the individual grains comprising the specimen. This applies especially for the plastic response of *hexagonal-close-packed* (*hcp*) metals, e.g. Ti, Mg, Zr or Be and their alloys, where at least 7 or more slip systems can be activated depending on the particular grain orientation and the grain surroundings [3-7].

A CP-Ti plate with an initial grain size of ~85 μm was hot rolled in a single pass at 720ºC to a reduction of 10% and water quenched to preserve the dislocation substructure. The setup of the diffraction experiment at the ID11 beamline at ESRF is shown in Fig. 1. The diffracted images were recorded at close- and far-detector positions. The close-detector position images were used

to determine the orientations of the individual grains in the specimen and to assign each diffraction spot to its grain of origin. This procedure was carried out by using the ImageD11 software [8]. The high angular resolution required for line profile analysis was achieved in the far-detector position, a typical image from which is shown in Fig. 2. The diffraction spots in these images were first located for the purpose of integration along the two "rocking-curve" directions, ω and η, defined in Fig. 2. After integration along these two directions, diffraction profiles in the radial, 2θ, direction are obtained. The integration volume was determined by an image recognition software developed specifically for the present work [S3]. Four selected ω frames with $\Delta\eta$ and $\Delta(2\theta)$ boundaries for a peak ranging over 7 subsequent ω frames are shown in Fig. 3. The integrated peaks were correlated to the diffraction spots on the close detector positions and in order to be associated with the different individual grains. The results of this evaluation procedure consist of diffraction patterns corresponding to different individual grains in the specimen together with the orientation of the grains in the specimen coordinate system. Fig. 4 shows typical reconstructed diffraction profiles with the corresponding *hk.l* indices.

It is usually a good assumption that only a limited number of slip systems with a limited number of Burgers vectors are active in each individual grain during deformation. This implies that the diffraction peaks corresponding to one grain should not be treated as the peaks of a "powder pattern". Rather, each profile is essentially a "single-crystal" peak.

The convolutional-multiple-whole-profile (CMWP) software, which was developed for the purpose of line profile analysis [9], has the option to assign individual dislocation contrast factors, C_{ind}, to each peak separately. These are thus considered as the measured values of

contrast factors, C_{ind}^{meas}. The contrast factors corresponding to different slip systems and different dislocations within each slip system can be calculated theoretically for the different *hk.l* values and are denoted as $C_{theo}(hk.l)$ [10]. The most-highly activated slip systems are then determined by matching the measured and theoretical contrast factors using an optimization process based on calculation of the sum of squared residuals (SSR) for all possible slip systems:

$$\sum_g \left(\frac{C_{theo}(g,n)}{C_{ind}^{meas}(g)} K - 1\right)^2 = min(n) = SSR(n)\ , \qquad (1)$$

in which *n* stands for the number of possible slip systems; in the present case, *n* = 7 (see table 1) [3, 4]. K is a scaling factor needed to match the measured, C_{ind}^{meas}, and the theoretically calculated, C_{theo}, contrast factors, and it is used to determine the dislocation densities in the individual grains. For a given grain, seven *SSR(n)* values are obtained. The selection of a particular most-highly activated slip system is considered unequivocal if one of the seven *SSR(n)* values is considerably less than all the others. The diffraction data of approximately 100 grains was evaluated by this means. For 49 of these grains, the *SSR*(n) values revealed a deep minimum, thereby clearly indicating the most-active slip system.

Strain broadening in a dislocated crystal is determined by the mean square strain [11]:

$$<\varepsilon_{g,L}^{\ 2}> = \frac{\rho C b^2}{4\pi} f(\xi)\ , \qquad (2)$$

where g and L are the diffraction vector and the Fourier variable of a peak profile, ρ and b are the dislocation density and the Burgers vector. $f(\xi)$ is the Wilkens function with $\xi=L/R_e$, where R_e is the effective outer cut-off radius of dislocations. The measured values of the dislocation contrast factors, C_{ind}^{meas} are evaluated by running the CMWP program with formal input values of the dislocation density ρ^* and b^*, as they appear as a product with the contrast factors in the mean square strain. The theoretically calculated, C_{theo}, and measured contrast factors are matched to each other by a scaling factor K as defined in eq. (1). The physically true dislocation densities, ρ_{ph} are finally obtained as:

$$\rho_{ph} = \frac{\rho^* b^{*2} K}{b_{ph}}, \qquad (3)$$

where b_{ph} are the physically true Burgers vectors. The values of b_{ph} are obtained once the most-active slip systems have been determined by evaluating equation (1).

The qualitative behavior deduced through the present procedure is shown by the Williamson-Hall (WH) and *modified* Williamson-Hall plots [2] in Fig. 5. The breadths of the peaks vary strongly when irradiating the same grain from different directions. This effect is caused by specific dislocations/slip directions prevailing in the grain. The variation of peak breadths is caused by the anisotropic diffraction contrast in different *hk.l* directions, similar to that observed in transmission electron microscopy (TEM). This anisotropic diffraction contrast is used to determine slip activity as in the case of Burgers vector analysis in TEM.

The orientations of the *c*- axes of the 49 investigated grains relative to the normal direction of the rolled plate are shown in Fig. 6. The distribution of the c axes is in good agreement with the overall texture of the specimen [12]. The frequency of the most-active slip systems in the different individual grains is shown in Fig. 7. The dislocation densities associated with most-active slip systems in the individual grains are shown in Fig. 8. The flow stress calculated using the total dislocation density ($\sigma=\alpha Gb\sqrt{\rho}$) is in a good agreement with the flow stress values of CP-Ti deformed in compression at 720°C [13]. Particularly, the experimental flow stress (at true strain of -0.12 and 718°C) in the RD and TD directions for polycrystalline CP-Ti was ~ 90 and 60 MPa, respectively, while the calculated flow stress is 61 MPa assuming $\alpha=0.5$, G=30.8 GPa, b=0.295 nm, and a total dislocation density $<\rho>=1.85 \times 10^{14}$ m^{-2}. A more accurate comparison requires dislocation densities from a much larger number of grains.

The Schmid factors (assuming Sachs' model) for the most-active slip systems determined here, assuming homogeneous plane-strain compression of an isotropic material, varied between 0.1 and 0.5. However, the stress state generated within a grain in a polycrystalline aggregate due to the constraint imposed by its neighbors can be very different from the macroscopic stress state [5-7]. Sophisticated modeling methods (e.g. finite element modeling (FEM) of crystal plasticity methods [5]) are necessary to determine the effect of neighboring grains on the stress state within each grain. Such modeling is outside the scope of this work, but to lay the groundwork for future modeling efforts we back-calculated, for each grain, the orientation in the sample coordinate system of the local normal stress that maximized the Schmid factor on the most-active slip system as determined by the present X-ray analysis (Figs. 9 and 10).

The X-ray line profile analysis method developed here provides active slip systems, Burgers vectors, and dislocation densities in individual grains in a polycrystalline aggregate, and is of particular interest for metals and alloys, structural materials, ionic crystals, or minerals constituting the earth's crust (for letter see reference [6]). The results obtained can be used either as input for sophisticated crystal-plasticity models, such as the visco-plastic-self-consistent- (VPSC) code [6,7] and the crystal-plasticity finite-element method (CPFEM) [5], or for experimental verification of the results of such numerical calculations.

Slip-system and Burgers vector analysis on the grain level in polycrystalline aggregates has been so far the domain of electron microscope methods, especially transmission electron microscopy (TEM). The method developed and demonstrated here complements and expands on what TEM offers. There are obvious similarities and differences between the TEM and X-ray procedures, both, experimentally and theoretically. In both cases the analysis is based on the different contrast effects produced by dislocations for different diffraction conditions. However, in a TEM experiment individual dislocations in selected grains are analyzed in great detail whereas in the X-ray procedure, although single grains can be investigated, the whole dislocation structure in the entire grain is studied at one time. The concomitant similarities and differences open up new perspectives for obtaining a more comprehensive insight into the microstructure of crystalline materials in terms of active slip-systems, Burgers vectors and dislocation densities. Finally, the X-ray procedure can also work under conditions when the TEM method cannot be applied, especially under non-ambient high-pressure conditions.

References

1. D. Juul Jensen, E. M. Lauridsen, L. Margulies, H. F. Poulsen, S. Schmidt, H. O. Sørensen and G. B. M. Vaughan, *Materials Today*, **9**, 18 (2006).
2. T. Ungár, A. Borbély, *Appl. Phys. Lett*. **69**, 3173 (1996).
3. P.G. Partridge, *Metallurgical reviews*, **118**, 169 (1968).
4. I. P. Jones, W. B. Hutchinson, *Acta Metall*. **29**, 951 (1981).
5. M.P. Miller, J.-S. Park, P.R. Dawson, T.-S. Han, *Acta Mater*. **56**, 3927 (2008).
6. S. Merkel, C. N. Tomé, H.-R. Wenk, *Phys. Rev. B*, **79**, 064110 (13) (2009).
7. R. A. Lebensohn, C. N. Tome, P. Ponte Castaneda, *Phil. Mag*. **87**, 4287 (2007).
8. J. Wright, ImageD11, http://sourceforge.net/projects/fable/files/ImageD11/
9. G. Ribárik, T. Ungár, J. Gubicza, *J. Appl. Cryst*. **34**, 669 (2001).
10. A. Borbély, J. Dragomir-Cernatescu, G. Ribárik, T. Ungár, *J. Appl. Cryst*. **36**, 160 (2003).
11. M. Wilkens, in *Fundamental Aspects of Dislocation Theory*, eds. Simmons, J.A., de Wit, R., Bullough, R., Vol. II. Nat. Bur. Stand. (US) Spec. Publ. No. 317, Washington, DC. USA, pp. 1195 (1970).
12. T. Ungár, M. G. Glavicic, L. Balogh, K. Nyilas, A. A. Salem, G. Ribárik, S. L. Semiatin,. *Mat. Sci. Eng. A*, **493**, 79 (2008).
13. A. A. Salem, S. R. Kalidindi, R. D. Doherty, M. G. Glavicic, S. L. Semiatin, in *Ti-2003 Science and Technology*, Wiley-WCH, Weinheim, Germany, pp. 1429 (2004).
14. N. E. Paton, W. A. Backofen, *Metallurgical Transactions*, **1**, 2839 (1970).
15. T. Xiaoli, G.U. Haicheng, Z. Shufen, C. Laird, *Mat. Sci. Eng. A*, **189**, 77 (1994).
16. M. H. Yoo , S. R. Agnew, J. R. Morris, K. M. Ho, Mat. Sci. Eng. A, 319, 87 (2001).

17. A. Snigirev, I. Snigireva, G. B. M. Vaughan, J. Wright, M. Rossat, A. Bytchkov, C.Curfs, *Journal of Physics: Conference Series*, **186**, 012073 (2009).

18. J. C. Labiche, O. Mathon, S. Pascarelli, M. A. Newton, G. G. Ferre, C. Curfs, G. B. M. Vaughan, A. Homs and D. F. Carreiras, *Review of Scientific Instruments*, **78**, 11 (2007).

19. B. Jakobsen, H. F. Poulsen, U. Lienert, J. Almer, S. D. Shastri, H. O. Sørensen, C. Gundlach, W. Pantleon, *Science*, **312**, 889 (2006).

20. Supported by the Hungarian National Science Foundation, OTKA T-71594 & T-67692. We thank the ESRF for allocation of beam time under the user program.

Supporting online materials

S1. T. Ungár, *The dislocation model of strain anisotropy*, the Hanawalt lecture given at the Denver X-ray Conference in Colorado Springs in 2007

S2. T. Ungár, G. Ribárik, L. Balogh, *Single grain microstructure from polycrystalline materials*, a lecture given at the Denver X-ray Conference in Colorado Springs in 2009

S3. G. Ribárik: http://www.renyi. hu/cmwp

Table 1. The most frequent slip systems of *hcp* titanium [3,14-16].

Slip-system notations	Burgers vectors	Slip planes	Total number of slip directions
Pr <*a*>	<-12-10>	{10-10}	3
B <*a*>	<-2110>	{0001}	3
Py I < *c*+*a* >	<-2113>	{10-11}	12
Py II < *c*+*a* >	<-2113>	{11-21}	12
Py III < *c*+*a* >	<-2113>	{2-1-12}	6
S <*a*>	<2-1-10>	-	3
S < *c*+*a* >	<-2113>	-	6

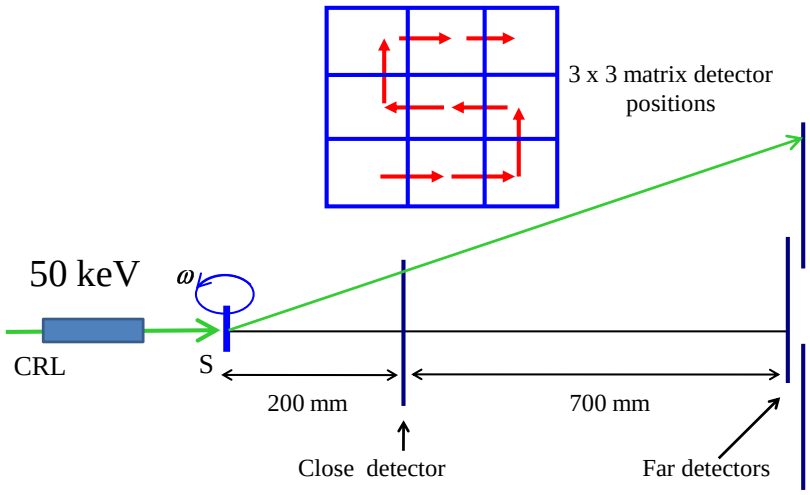

Figure 1. Schematic setup of the diffraction experiment at the ID11 beamline of the ESRF synchrotron in Grenoble, France. A thin, needle-shaped sample of 0.2-mm diameter and 12-mm length (shown as a short blue line, denoted as "S" in the figure) was cut by a diamond saw and electropolished. The long direction of the sample was parallel to the normal direction of the hot rolled plate. The specimen was placed in an ω goniometer on an x-y-z stage in front of the X-ray beam. The beam was focused at the sample to 50 μm in the vertical and 400 μm in the horizontal direction by a compound refractive lens (CRL), with a focal length of approximately 4 m [17]. The scattered radiation was detected by fibre-optic coupled FReLon area detector [18] having a 50 μm pixel size and a 100×100 mm aperture. A distance from the specimen to the detector is either 200 mm in the *close-detector* mode or 700 mm in the high resolution *far-detector* mode. The detector locations are shown schematically as dark blue lines in the close and far positions. In the far-detector mode, the detector was moved sequentially to 9 different positions in a 3×3 matrix indicated by red arrows in order to cover a large area in reciprocal space. The specimen was rotated around the ω axis, more detailes are given in Fig. 2.

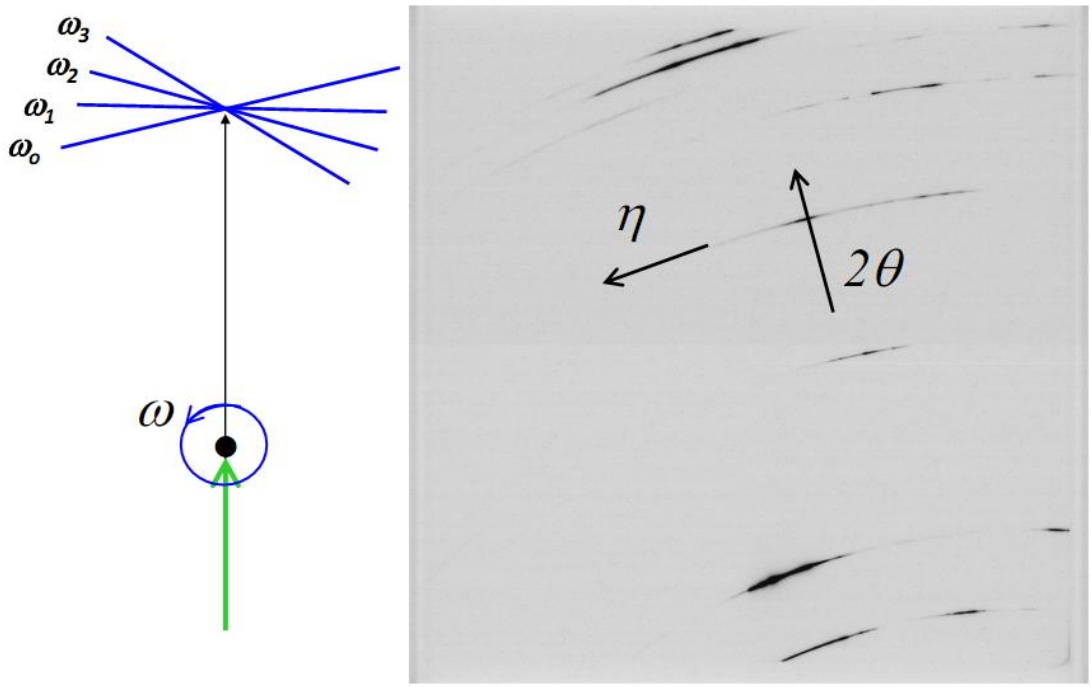

Figure 2. A typical image of a far-detector frame along with a schematic drawing of the ω movement of the specimen looking down on the plane of incidence.The specimen was rotated around the ω axis by $\Delta\omega=0.2^{o}$ or 0.5^{o} steps over $\pm 60^{o}$ in the close- and the far-detectors modes, and the diffraction patterns were measured in each ω setting for 1 or 8 seconds, respectively. 600 frames were recorded in the far-detector mode in each of the 3×3 detector positions. The diffraction peaks are elongated along the Debye-Scherrer arcs in the η direction and broadened in the radial 2θ direction, typical for crystals or grains containing dislocations [19].

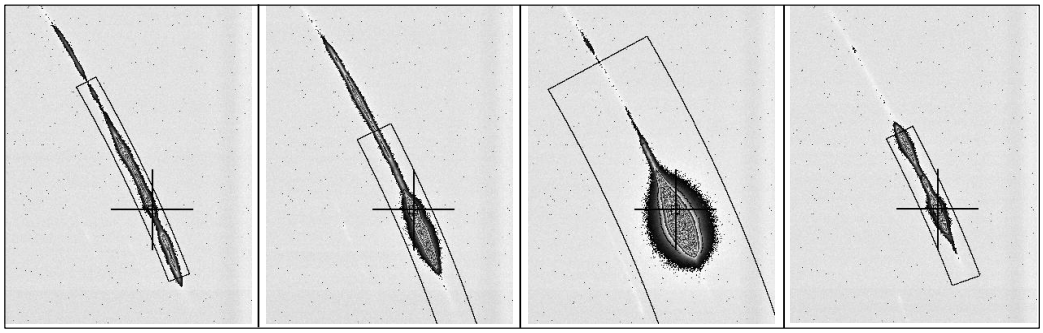

Figure 3. Portions of four typical far-detector frames showing the integration procedure along the Debye-Scherrer arcs in the η direction. The large crosses mark the highest intensity positions in the frames and the lines circumventing the diffraction spots are placed at distances of ±6-times and ±15-times the full-width-at-half-maximum (FWHM) of the peaks in the radial, i.e. 2θ, and in the η directions, respectively. Integration over the ω direction is done by summing up the frames over an ω range where the intensity falls off to 1% of the maximum intensity. For the peak shown here 7 subsequent ω frames have been summed up. After integration along the η and ω directions diffraction profiles in the radial, i.e. the 2θ, direction are obtained. Image recognition software has been developed for the present specific case and will be available for similar experiments through the web [S1].

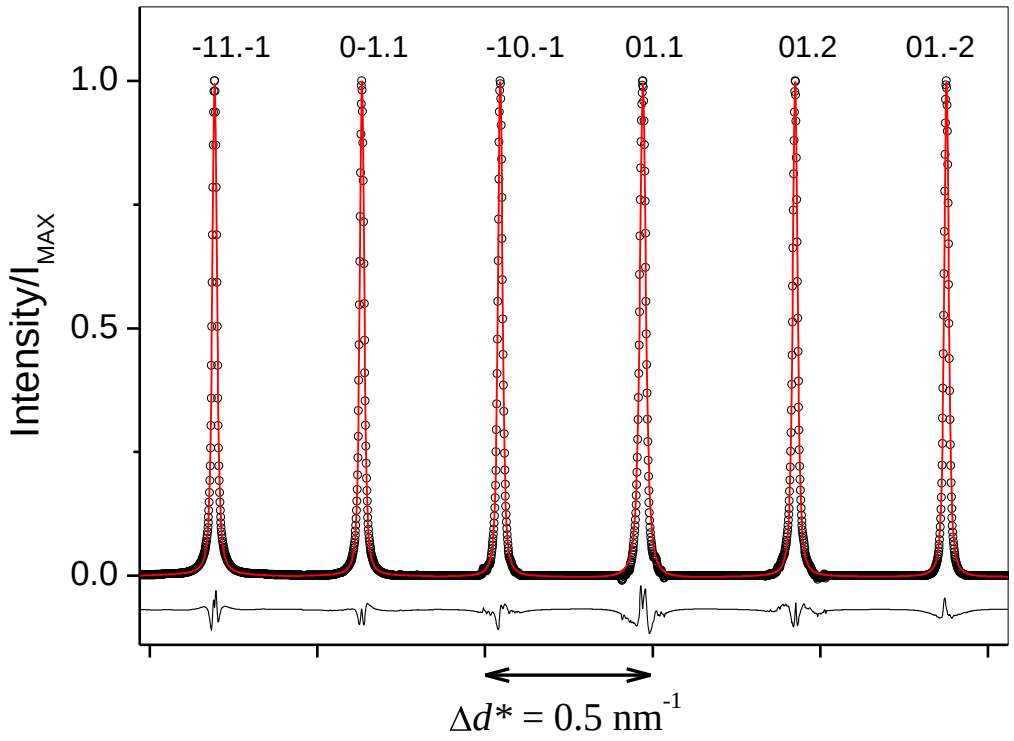

Figure 4. Typical diffraction profiles corresponding to one particular single grain inside the bulk polycrystalline specimen. The open circles are the measured points, and the red line is the fitted profile determined by the line-profile analysis software CMWP [9]. The second, third, and fourth (i.e. $0\bar{1}.1$, $\bar{1}0.\bar{1}$ and 01.1) lines and the two last lines (i.e. 01.2 and $01.\bar{2}$) each correspond to a given *d* value but to different specific directions in the same family of planes, since the measured Bragg reflections were generated by a single grain or crystal in the bulk polycrystalline aggregate. Accordingly, the scale is given as Δd^* (where $d^*=2\sin\theta/\lambda$) to indicate the breadths of the peak profiles. The thin line below the spectra is the difference between the measured and fitted intensities.

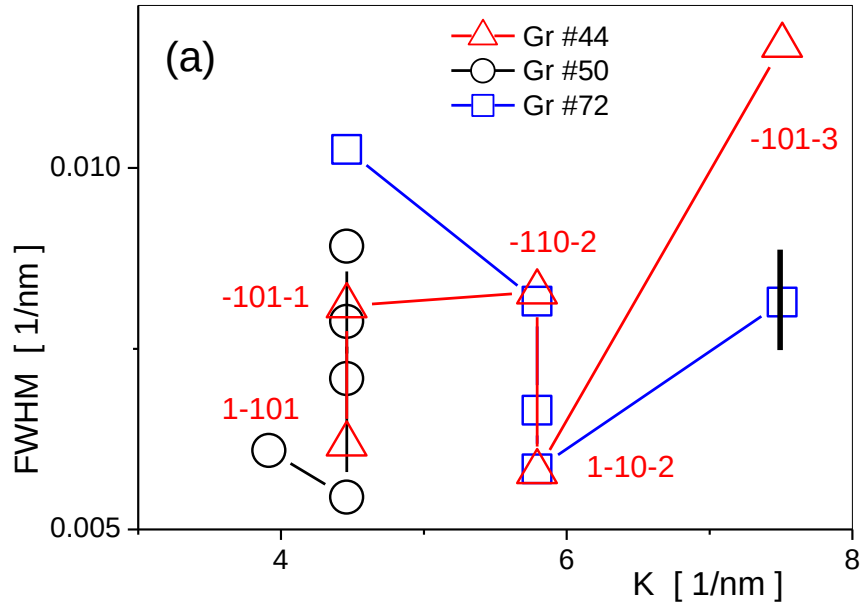
(a)
Gr #44
Gr #50
Gr #72
-101-3
-110-2
-101-1
1-101
1-10-2
0.010
0.005
FWHM [1/nm]
4
6
8
K [1/nm]

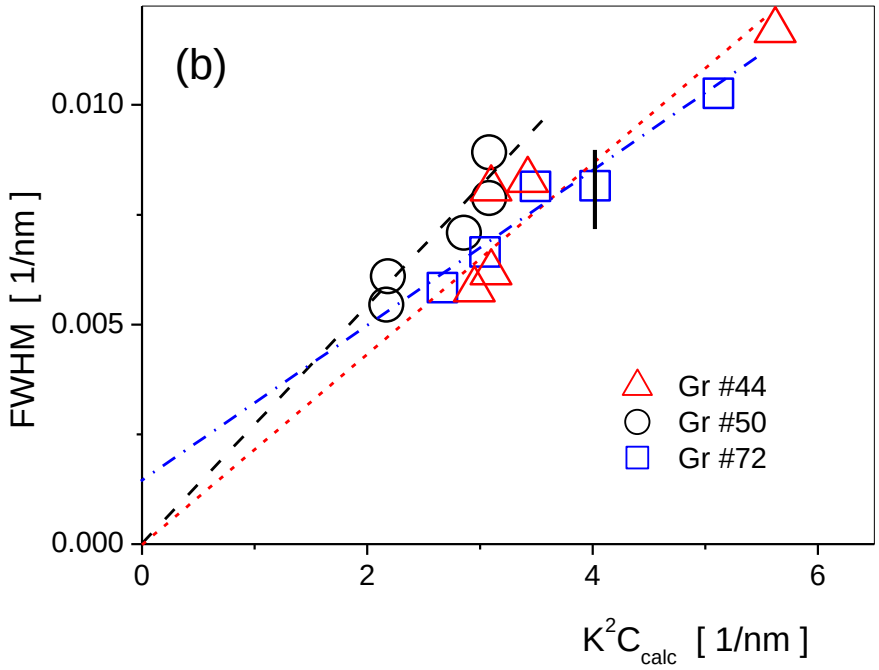
(b)
0.010
0.005
0.000
FWHM [1/nm]
Gr #44
Gr #50
Gr #72
0
2
4
6
K2Ccalc [1/nm]

Figure 5. The FWHM (in 1/nm scales) in Williamson-Hall (a) and *modified* Williamson-Hall (b) plots [2] for three typical grains. The *hk.l* indices are given for grain #44 in (a), others are not shown in the figure for clarity. Strain anisotropy is obvious in (a), i.e. the breadths are very different for different orientations in the same grain indicating that only a few specific dislocations are present in each grain. Strain anisotropy is clarified in the *modified* Williamson-Hall plot (b) by using the theoretical contrast factors, C_{calc} for the dislocations in the most-active slip system, i.e. Screw <*c*+*a*> in grain #44, Pyramidal < *c*+*a* > in grain #50 and Prismatic <*a*> in grain #72; the corresponding slip planes and Burgers vectors are listed in Table 1. The dash or dash-dot lines are linear fits to the data. The small or zero intercepts of these lines at $K^2C_{calc}=0$ are in correlation with the fact that, in the present case, practically no size effect contributes to peak broadening.

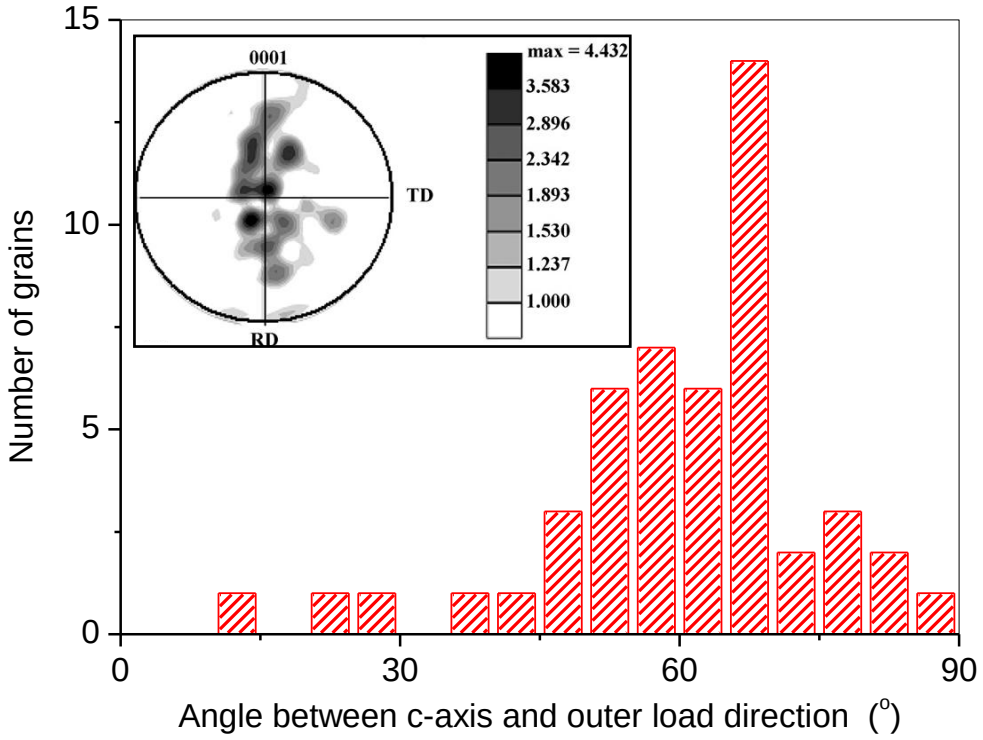

Figure 6. The orientations of the *c*- axes in the *hcp* lattice of the 49 investigated grains relative to the normal direction of the rolled plate. The collection of grain orientations around approximately 50 to 70^{o} is consistent with the texture of the hot rolled plate [12] shown in the inset, where RD is the rolling direction and TD the transverse direction.

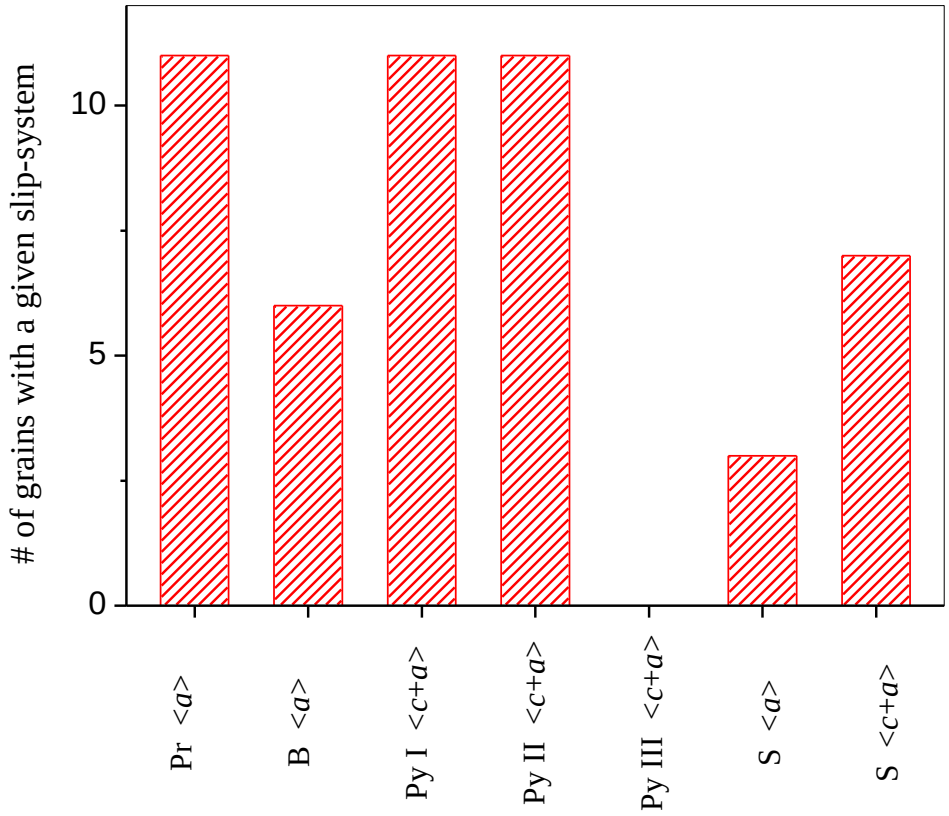

Figure 7. The frequency of the most-active slip systems in the different individual grains. The key for the short notations of the slip-plane types with the Burgers vector types, the slip plane normal and the number of possible dislocations within each slip-system types are given in Table 1. In 29 out of the 49 investigated grains, the prevailing slip is of <*c*+*a*> type and in the rest <*a*> type in correlation with TEM observations and theoretical calculations [3,14-16]. <*c*> type slip has not been found in any grain.

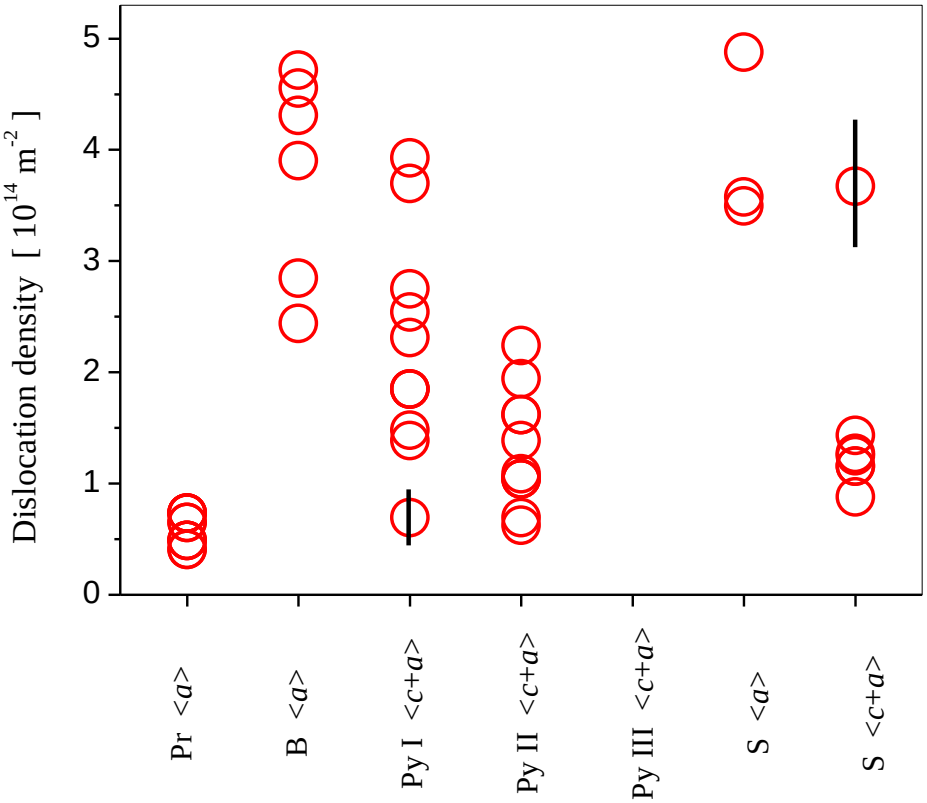

Figure 8. The dislocation densities in the different individual grains determined by assuming that the Burgers vectors are those associated with the most-active slip systems. The average dislocation densities in all the grains, $\rho_{total}=1.85\times10^{14}$ m^{-2}, and in the grain populations where the most-active slip systems are either of <*a*> or of <*c*+*a*> type, i.e. $\rho_{<a>}=2.2\times10^{14}$ m^{-2} or $\rho_{<c+a>}=1.62\times10^{14}$ m^{-2}, respectively. (In all ρ values the experimental error is $\pm0.2\times10^{14}$ m^{-2}.)

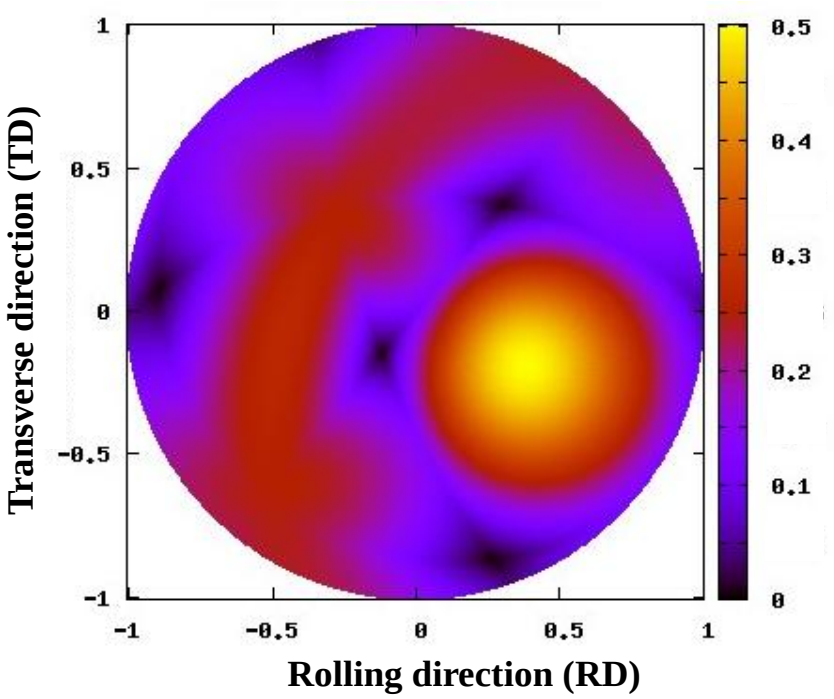

Figure 9. An example of a calculation of the orientation of the normal stress maximizing the Schmid factors on a specific slip system within a given crystal orientation. The most-active slip system and the grain orientation were first determined by the current X-ray line profile analysis method. Schmid factors were then calculated for all possible stress orientations acting on the measured slip system. On a stereographic projection of Schmid factors, the normal stress with Schmid factor of 0.5 (yellow color) was determined. Repeating the process for all grains and the associated most-active slip systems results in Fig.10.

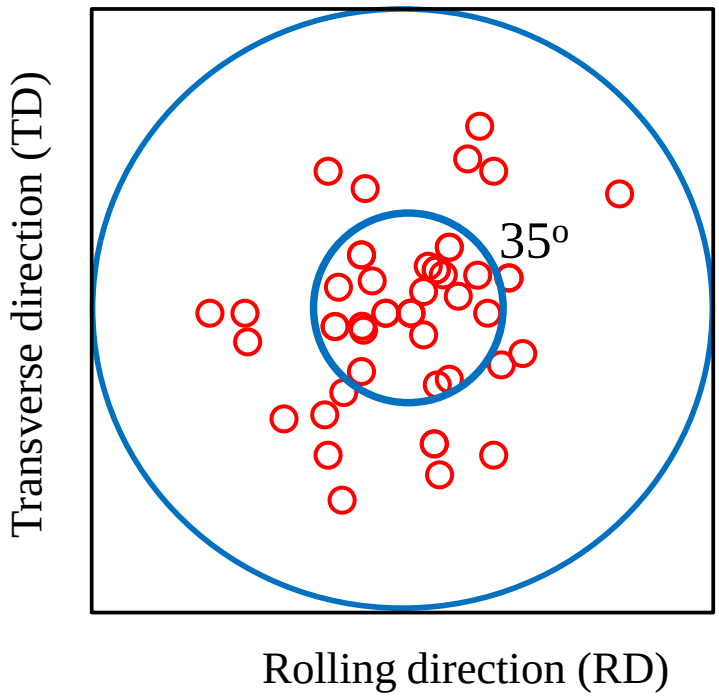

Figure 10. Stereographic projection of the normal stresses with average Schmid factors between 0.4 and 0.5 on the most-active slip systems within all investigated grains, determined using the procedure described in Fig 9. For almost 70% of the grains, normal stresses with a Schmid factor of close to 0.5 on the most active slip system were tilted within 35^{o} from the ND of the rolled plate (bounded by the small circle in the figure). The results in Figs. 9 and 10 provide a wealth of information for validating future crystal plasticity modeling efforts that will include the effect of neighboring grains on stress states in polycrystalline hcp material.